Solid Lewis Acids Catalyze the Carbon–Carbon Coupling between Carbohydrates and Formaldehyde

Stijn Van de Vyver, Caroline Odermatt, Kevin Romero, Teerawit Prasomsri, and Yuriy Román-Leshkov*

Department of Chemical Engineering, Massachusetts Institute of Technology, Cambridge, Massachusetts 02139, United States

S Supporting Information

ABSTRACT: The development of catalytic C–C bond formation schemes based on renewable substrates is important for defining sustainable paradigms for chemical manufacturing. With a few exceptions, aldol condensation reactions between biomass-derived platform chemicals have received little attention so far. Here the C–C coupling between 1,3-dihydroxyacetone (DHA) and formaldehyde into α-hydroxy-γ-butyrolactone (HBL) using Sn-Beta is demonstrated. Reactivity studies, coupled with spectroscopic and computational analyses, show that the formation of HBL proceeds by soft enolization of DHA followed by an aldol addition of formaldehyde to the Sn-enolate intermediate, generating erythrulose as an intermediate species. Isotopic labeling is used to reveal the position where formaldehyde is incorporated into HBL, providing further support for our proposed mechanism. Finally, combining the C–C coupling reaction with transfer hydrogenation of formaldehyde has allowed us to expand the substrate scope to include polyols glycerol and ethylene glycol.

KEYWORDS: aldol condensation, biomass conversion, heterogeneous catalysis, isotope labeling studies, proton transfer, Sn-Beta, soft enolization, solid Lewis acid
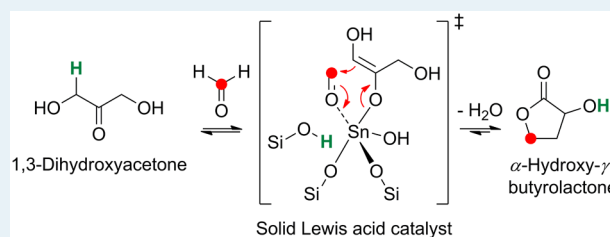
Metal centers with open coordination sites incorporated into the framework of zeolites have attracted significant attention as Lewis acid catalysts due to their ability to activate hydroxyl and carbonyl functional groups.[1−3] For example, Sn sites incorporated into a defect-free framework with the BEA topology (Sn-Beta) have shown remarkable activity for transformations such as the Meerwein−Ponndorf−Verley (MPV) reduction of aldehydes and ketones,[4−7] the etherification of alcohols,[4,8] and the Baeyer−Villiger oxidation of ketones to lactones.[9,10] Despite the prevalence of homogeneous acid and base catalysts for aldol condensation reactions,[11] the use of solid Lewis acids remains largely unexplored. Few exceptions include the observation of Sn-catalyzed aldol condensation of glycolaldehyde in the synthesis of methyl-4-methoxy-2-hydroxybutanoate, methyl lactate, or vinyl glycolate esters.[12,13] Sn-Beta and other Sn-containing silicates have also been used for C–C bond formation reactions such as the intramolecular cyclization of citronellal to isopulegol[14] and the intermolecular Prins reaction between β-pinene and paraformaldehyde for the formation of nopol.[15−18]

Here we show the first application of Sn-Beta for the catalytic C–C coupling between triose sugars and formaldehyde to form α-hydroxy-γ-butyrolactone (HBL), which is an important chemical intermediate used for production of herbicides[19] and pharmaceutical agents.[20−22] Previously, HBL has been synthesized by radical coupling between 1,3-dioxoranes, acrylates, and molecular oxygen,[21] or by alkylation, hydrolysis, and cyclization of hydroxy-4-methylthiobutyric acid.[22] More recently, Yamaguchi et al. reported the direct catalytic

transformation of 1,3-dihydroxyacetone (DHA) and formaldehyde into HBL in the presence of tin(IV) chloride.[23] For this reaction, however, the mechanism remains unclear, particularly on how the enolization and proton transfer steps are promoted by the Sn centers. Also, there is a significant drive to develop heterogeneous catalysts to avoid additional energy-intensive separation and recovery steps, as well as irreversible deactivation upon interacting with water.[24]

Table 1 shows results for C–C coupling reactions between DHA and formaldehyde catalyzed by solid Lewis acids. Reactivity studies were performed in batch reactors at 160 °C using 1,4-dioxane as solvent, paraformaldehyde as the formaldehyde source, a metal/DHA ratio of 1:100 and a DHA/formaldehyde ratio of 1:3. Sn-Beta showed the highest selectivity of all Beta zeolites studied, generating an HBL yield of 60% at 98% conversion after 3 h (entry 1).[25] Byproducts observed were lactic acid (LA) and (1,3-dioxolan-4-yl)methanol (Supporting Information, Figure S1), with the latter formed by acetalization of formaldehyde with DHA.[26] Previous studies have indicated the promoting effect of water on the catalytic activity of SnCl₄.[23] In our study, small amounts of water were found to increase the solubility of paraformaldehyde as well as the HBL yield (entry 2). The results given in Table 1 further indicate that Sn is the optimal metal for the present reaction, as Zr-, Hf-, Ti-, and Al-Beta showed drastically

Table 1. Results for the Lewis Acid Catalyzed Synthesis of HBL[a]

entry	catalyst	Si/metal ratio[b]	substrate	conv. [%]	yield[c] [%]		
					HBL	LA	1,3-DIOXO derivatives
1	Sn-Beta	98	DHA	98	60	9	17
2	Sn-Beta[d]	98	DHA	98	68	8	18
3	Sn-Beta	98	ethylene glycol	98	13	1	47
4	Sn-Beta	98	glycerol	98	12	10	52
5	Zr-Beta	111	DHA	99	3	2	8
6	Hf-Beta	112	DHA	99	7	3	12
7	Ti-Beta	140	DHA	96	6	3	3
8	Al-Beta	13	DHA	95	11	6	9
9	Sn-MCM-41	117	DHA	99	64	15	5
10	Sn-MFI	180	DHA	90	61	6	4
11	SnO_2/Si-Beta	100	DHA	53	3	<1	<1
12	none	−	DHA	12	<1	<1	<1

[a]Reaction conditions: 2.4 mmol substrate, 7.2 mmol paraformaldehyde, 8 mL 1,4-dioxane, 0.024 mmol metal in added catalysts, 20 bar Ar at RT, 160 °C, 3 h. [b]Determined by inductively coupled plasma atomic emission spectrometry (ICP-AES). [c]Determined by GC/FID and expressed relative to the initial molar amount of DHA. 1,3-DIOXO derivatives = (1,3-dioxolan-4-yl)methanol and other substituted 1,3-dioxolane derivatives. [d]Reaction performed in the presence of 2.4 mmol water.

Scheme 1. Proposed Mechanistic Pathway for the C−C Coupling between DHA and Formaldehyde Catalyzed by the Framework Lewis Acidic Sn Sites in Sn-Beta[a]
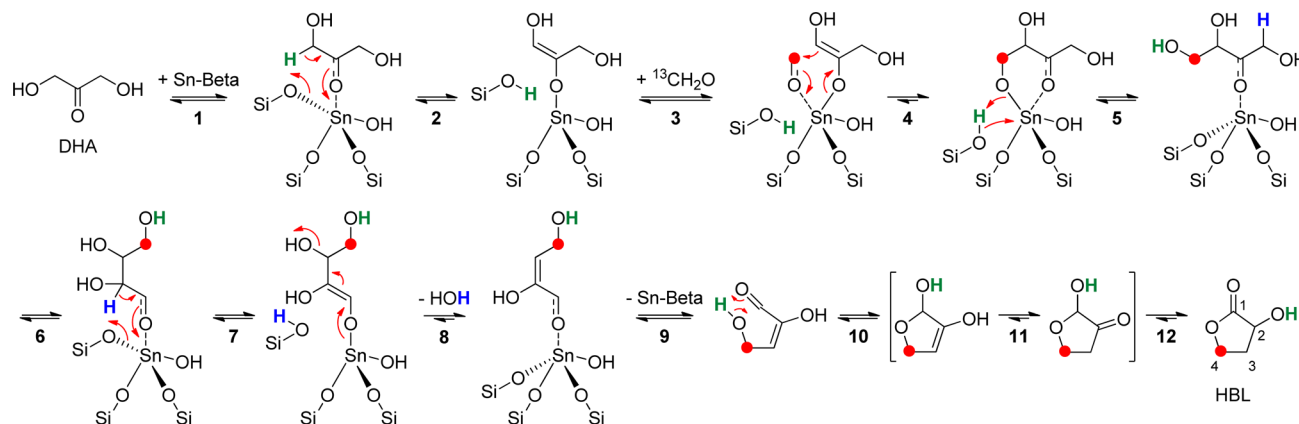
[a]H atoms involved in proton transfer and 1,2-hydride shift steps are marked in green and blue. ^{13}C atoms are shown as red dots.

lower HBL yields (entries 5−8). These catalysts, however, were found to promote side reactions originating from the high reactivity of formaldehyde. Other Sn-containing catalysts, such as Sn incorporated into a mesoporous, amorphous framework (Sn-MCM-41; entry 9) or stannosilicate zeolites with MFI topology (Sn-MFI; entry 10)[27] generated comparable HBL yields to those obtained with Sn-Beta. From a mechanistic point of view, it is important to note that extra-framework SnO_2 nanoparticles impregnated on Si-Beta (SnO_2/Si-Beta) showed no significant activity in generating HBL (entry 11). Finally, we confirmed that the reaction does not occur in the absence of DHA or formaldehyde, and that similar HBL yields can be obtained when using glyceraldehyde as substrate.

The proposed reaction pathway for the C−C coupling between DHA and formaldehyde is depicted in Scheme 1. We hypothesize that the critical aldol addition step is catalyzed by Sn-Beta through a soft enolization process,[28] wherein the Lewis acidic Sn site acts in concert with the weakly basic oxygen atom in the framework Si−O−Sn ensemble to deprotonate DHA.[29] More specifically, in our proposed mechanism, the Lewis acidic framework Sn atom polarizes the carbonyl group of DHA, resulting in a substantial increase in the acidity of the α-proton (Step 1). This proton can consequently be removed by the

basic oxygen atom connected to Sn, generating a Sn-enolate intermediate and a silanol group (Step 2). Coordination of the oxygen atom of formaldehyde to the Sn center induces polarization in the molecule, further enhancing its reactivity by increasing the electrophilicity of the aldehyde carbon (Step 3).[24] Aldol addition of formaldehyde to the Sn-enolate intermediate (Step 4), followed by proton transfer from the silanol of the active site to the oxygen atom at the C4 position (Step 5), results in formation of erythrulose. The erythrulose produced this way can then isomerize into erythrose through a 1,2-hydride shift similar to that observed during glucose−fructose isomerization with Sn-Beta (Step 6, intermediate steps are not shown for simplicity).[30] The presence of the carbonyl and β-hydroxyl group in erythrose makes it highly susceptible to dehydration via a retro-Michael reaction (Steps 7 to 8).[13,31,32] We speculate that both the proton transfer step to form the Sn-enolate intermediate and β-elimination of the hydroxyl group can be mediated by Sn-Beta. Alternatively, erythrose dehydration may also proceed via classic Brønsted acid catalysis.[33] Subsequent cyclization of the retro-Michael product involves an intramolecular hemiacetal reaction (Step 10).[34] Lastly, a keto−enol tautomerization (Step 11) and a 1,2-hydride shift (Step 12) generate the desired HBL product.

The tentative mechanism is in agreement with previous experimental studies showing that Sn-Beta and $SnCl_4$ catalyze the following: (1) keto−enol tautomerization of DHA;[35,36] (2) retro-aldol fragmentation of sugars;[12,37] (3) isomerization of erythrulose to erythrose;[38] and (4) conversion of erythrose into HBL.[32] Although enolization has not been observed during glucose-fructose isomerization with Sn-Beta,[39] Dusselier et al. postulated a Lewis acid catalyzed self-aldol addition of glycolaldehyde in the cascade synthesis of C4 α-hydroxy acids using homogeneous Sn halides.[13] The mechanism shown in Scheme 1 is new in that Steps 2 and 7 involve the transfer of a proton from a C−H bond to the zeolite lattice. Recent computational studies on the catalytic activity of Sn-Beta support a similar role for the weak basic oxygen atoms connected to Sn in proton transfer reactions involved in the isomerization of glucose to fructose.[29] Another argument in favor of the hypothesized pathway is the spectroscopic observation that Si−O−M ensembles promote C−H activation, even in more challenging scenarios such as the initiation of ethylene polymerization.[40]

Formation of the aldol addition product erythrulose as a reaction intermediate in the production of HBL was substantiated by using it as a reactant in place of DHA. A reaction of erythrulose with Sn-Beta under identical conditions as those used for DHA generated a 24% HBL yield, thus confirming that erythrulose can undergo the suggested catalytic transformation. To further support the proposed mechanism, isotopically labeled formaldehyde was reacted with DHA in the presence of Sn-Beta and investigated using GC-MS and ^{13}C nuclear magnetic resonance (NMR). The mass spectrum of the product mixture is identical to that obtained from the reaction with unlabeled formaldehyde, but it is shifted by $m/z = 1$ to higher m/z ratios (Supporting Information, Figure S2). Specifically, the main fragment ion at m/z 58, corresponding to the resonantly stabilized species $^{13}CH_2$=CH−CH$^+$−OH,[41] indicates that HBL contains the ^{13}C label at the C4 position. This was corroborated by the ^{13}C NMR spectrum, which showed a main resonance at $\delta = 65.2$ ppm corresponding to the C4 atom (Figure 1a). The highly selective incorporation of ^{13}C atoms at the C4 position of HBL can indeed be rationalized by considering the proposed C−C bond formation mechanism (Scheme 1).

DFT-calculated standard-state enthalpy (ΔH°_{rxn}) and Gibbs free energy changes (ΔG°_{rxn}) for our mechanism (Scheme 1) and the one proposed by Yamaguchi et al.[23] are listed in Table S1 in the Supporting Information.[42] Formation of erythrulose is calculated to proceed exothermically with a ΔG°_{rxn} value of 0.4 kJ mol^{-1}, which, although slightly positive, compares favorably to 16.8 kJ mol^{-1} for the previously proposed aldol addition of formaldehyde to pyruvic aldehyde to form 4-hydroxy-2-oxobutanal.[23] The estimated ΔG°_{rxn} values of the ring closure and 1,2-hydride shift are −49.1 and −57.0 kJ mol^{-1}, respectively, strengthening the feasibility of the reaction mechanism shown in Scheme 1. Note that these values are calculated for gas phase reactions as the solvation effect is believed to be relatively small in the hydrophobic zeolite system.[29,43] Future periodic density functional and other quantum mechanical studies will be critical to accurately assess solvation contributions and binding energies of the substrates with the catalytic site.

To detect any possible carbohydrate products resulting from the C−C coupling between DHA and formaldehyde, aliquots taken from a standard reaction mixture at 3 h were derivatized
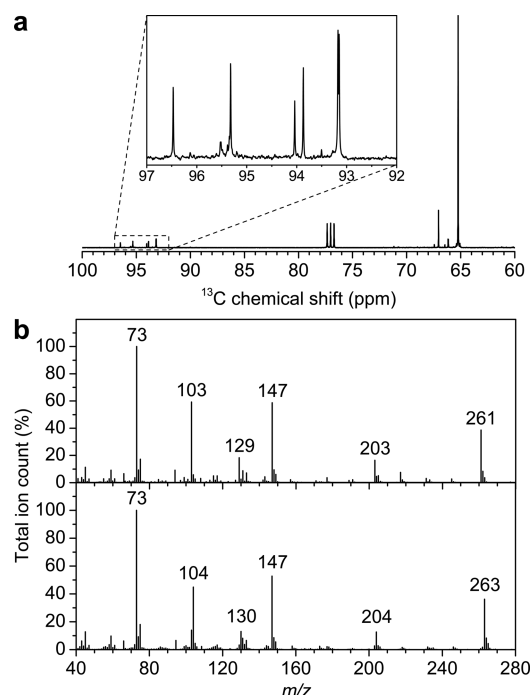

Figure 1. (a) 400 MHz ^{13}C NMR spectrum of the product mixture obtained after reacting [^{13}C]formaldehyde with DHA in the presence of Sn-Beta. (b) Mass spectra of the TMS-sugar derivatives obtained from reactions with unlabeled (top) and isotopically labeled formaldehyde (bottom).

by trimethylsilylation (TMS) and analyzed by GC−MS. A comparison of these mass spectra with those obtained from TMS derivatives of a reaction mixture using isotopically labeled formaldehyde shows that under the temperature and reaction times investigated, significant amounts of C5 sugars are obtained (Figure 1b). We infer that these sugars are formed by a second aldol addition of formaldehyde to the Sn-enolate form of erythrose in an analogous way to Steps 4 and 5 in Scheme 1. C4 and C5 aldose formation was tentatively confirmed by ^{13}C NMR spectroscopy, which showed resonances in the region between 90 and 100 ppm character-istic of the anomeric C1 atom (inset in Figure 1a).[44] Work is in progress to identify these products by fractionation of the reaction mixture and 2D NMR analysis. Importantly, negative control experiments—omitting one of the key components (formaldehyde, DHA or catalyst)—gave no observable sugar formation.

To expand the substrate scope of this reaction, we investigated the possibility of combining the C−C coupling with transfer hydrogenation in a cascade reaction sequence. Our previous studies showed that Lewis acid zeolites can catalyze one-pot cascade processes in which the MPV reduction of aldehydes occurs under the same reaction conditions as hydrolysis[6] or etherification reactions.[4] Here we demonstrate the sequential Sn-Beta catalyzed Oppenauer (OPP) oxidation/aldol condensation of ethylene glycol and glycerol, with formaldehyde functioning both as hydrogen acceptor and condensation reagent. Under identical conditions to those used for DHA, HBL could be formed with 12−13% yield at 98% conversion (Table 1, entries 3−4). In view of the mechanism outlined in Scheme 1, we anticipated that the cascade reaction could be initiated through hydrogen transfer between the alcohol and formaldehyde, resulting in the formation of DHA.

Interestingly, a similar process has been patented wherein Sn-Beta catalyzes the oxidation of vanillyl alcohol in an aqueous solution of formaldehyde.[45] As a proof-of-concept experiment, we performed a reaction of 2-hexanol with formaldehyde in the presence of Sn-Beta. GC/MS analysis of the reaction mixture showed formation of 1-hepten-3-one (Supporting Information, Figure S3), which can only be explained by a tandem OPP oxidation/aldol condensation of the formed 2-hexanone with formaldehyde catalyzed by Sn-Beta. In addition, we identified methyl formate as one of the byproducts, indicating the occurrence of a concomitant MPV reduction of formaldehyde into methanol.[46] The present reaction data, however, cannot exclude that dimerization of formaldehyde occurs through a Lewis acid catalyzed Tishchenko reaction,[47] thus requiring further studies for confirmation.

Table 2 shows the effect of the solvent and its dielectric constant (ε)[48,49] on the catalytic performance of Sn-Beta for

Table 2. Effect of the Solvent on the Catalytic Performance of Sn-Beta for the Reaction of DHA with Formaldehyde[a]

entry	solvent	ε[b]	conv. [%]	HBL yield [%]
1	1,4-dioxane	2.2	98	60
2	THF	7.5	99	49
3	GVL	37	>99	61
4	ethanol	25	89	1

[a]Reaction conditions: see Table 1. [b]Dielectric constants (ε) were obtained from refs 48 and 49.

the reaction of DHA with formaldehyde. Aprotic polar solvents such as tetrahydrofuran (THF) and γ-valerolactone (GVL) generate comparable yields to those obtained with 1,4-dioxane (Table 2, entries 2−3), while protic polar solvents such as ethanol lead to inferior HBL yields (1%; entry 4). GVL provides a promising alternative for 1,4-dioxane because of its favorable toxicological and physical properties.[50] Although not yet used industry-wide, it has recently attracted academic interest as a renewable solvent in acid-catalyzed biomass conversion reactions.[51,52] Note that the lack of selectivity in the case of ethanol is likely due to its tendency to competitively adsorb on Lewis acid centers, thereby hindering coordination of the reactants with the active site.[4,24]

The stability of Sn-Beta was investigated by simple recycling experiments in which the catalyst was separated by filtration, washed with acetone, dried, and calcined in air at 550 °C. Reusing Sn-Beta over three runs led to a decrease in HBL yield of 20% while the DHA conversion remained almost constant (Supporting Information, Figure S4). To investigate the deactivation pathways in more detail, we also tested the catalyst in a packed-bed flow reactor. In order to solubilize all reactants flowing into the packed bed, an aqueous form-aldehyde solution (37 wt %) was used instead of the dry polymeric paraformaldehyde. Figure 2 shows a plot of the catalytic activity of Sn-Beta as a function of time on stream (TOS). Under the conditions investigated, DHA conversion decreased from 95 to 87% over the course of 48 h. HBL yields stabilized between 34 and 36% after ca. 20 h on stream, then decreased slightly at longer times. The resulting average productivity was calculated to be approximately 18.1 g HBL per g catalyst per h. Significantly higher LA yields were obtained compared to the reactions performed under batch conditions, which can be attributed to the presence of water in the reactant solution. In contrast to the batch experiments,
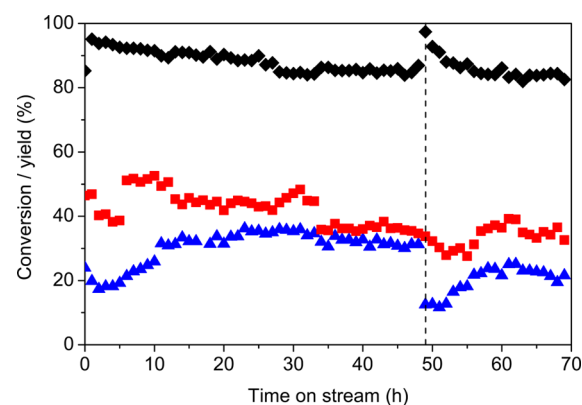

Figure 2. Evolution of the DHA conversion (black diamonds) and yields of HBL (blue triangles) and LA (red squares) as a function of TOS. Reaction conditions: 2.6 wt % DHA in dioxane, 2.6 wt % formaldehyde solution (37 wt % in H_2O with 10−15% methanol), 160 °C, 24 bar, weight hour space velocity of 35.6 h^{-1}, flow rate of 3.7 mL h^{-1}. Catalyst regeneration is indicated by the dashed line.

conversion levels were kept at ca. 90% in the flow reactor in order to track deactivation more accurately. Consequently, we found a more complex mixture of intermediates and oxy-genated molecules than that obtained in the batch reactors at the residence times shown in Table 1. To study the potential reactivation of Sn-Beta and infer its deactivation mechanism, regeneration of the catalyst was attempted by flushing the catalyst bed with 1,4-dioxane and in situ calcination in air at 550 °C for 5 h. After reactivation, we observed a deactivation profile similar to that of the original sample, but with reduced HBL yields (≤25%). After 70 h of operation, the catalyst was recovered and characterized by various techniques. Thermog-ravimetric analysis (TGA) of this material revealed a 5% weight loss over a temperature range of 150−600 °C (Supporting Information, Figure S5), indicating the adsorption of carbona-ceous components on the zeolite. N_2 physisorption measure-ments showed a decrease in micropore volume from 0.17 to 0.14 cm^3 g^{-1} (Supporting Information, Figure S6), suggesting that catalyst deactivation may, at least in part, be due to micropore collapse. However, this structural damage did not result in significant changes to the long-range topological order of the Beta zeolite as shown by powder X-ray diffraction (PXRD; Supporting Information, Figure S7).

In conclusion, we have demonstrated the C−C coupling between 1,3-dihydroxyacetone and formaldehyde using Sn-Beta as a solid Lewis acid catalyst. Remarkably, besides the main product HBL, we were able to observe the formation of C5 sugars, indicating the occurrence of two consecutive aldol addition reactions. Isotopic labeling studies corroborate a mechanism involving soft enolization of DHA followed by an aldol addition of formaldehyde to the Sn-enolate intermediate, generating erythrulose as an intermediate species. Moreover, combining the C−C coupling reaction with hydrogen transfer in a cascade sequence allowed us to extend this concept to polyols such as glycerol and ethylene glycol, which could ultimately be exploited in cellulose conversion schemes.[53] Our ongoing efforts to identify the aldose byproducts and to develop a deeper understanding of how the Lewis acid catalyzed aldol condensation occurs will be useful for the deliberate catalytic synthesis of carbohydrates larger than tetroses.

ASSOCIATED CONTENT

ⓢ Supporting Information

The following file is available free of charge on the ACS Publications website at DOI: 10.1021/cs5015964.

Experimental procedures for the catalyst synthesis, characterization and testing, details on the DFT calculations, GC/MS data of the product mixture formed in the Sn-Beta catalyzed reaction of DHA with formaldehyde, MS data of the products formed in the reaction with isotopically labeled formaldehyde and in the reaction with 2-hexanol, results of recycling experiments of Sn-Beta, TGA, N_2 physisorption and PXRD data (PDF)

AUTHOR INFORMATION

Corresponding Author

*E-mail: yroman@mit.edu.

Notes

The authors declare no competing financial interest.

ACKNOWLEDGMENTS

REFERENCES

(1) Moliner, M. *Dalton Trans.* **2014**, *43*, 4197−4208.

(2) Gunther, W. R.; Michaelis, V. K.; Caporini, M. A.; Griffin, R. G.; Román-Leshkov, Y. *J. Am. Chem. Soc.* **2014**, *136*, 6219−6222.

(3) Corma, A.; Garcia, H. *Chem. Rev.* **2002**, *102*, 3837−3892.

(4) Lewis, J. D.; Van de Vyver, S.; Crisci, A. J.; Gunther, W. R.; Michaelis, V. K.; Griffin, R. G.; Román-Leshkov, Y. *ChemSusChem* **2014**, *7*, 2255−2265.

(5) Luo, H. Y.; Consoli, D. F.; Gunther, W. R.; Román-Leshkov, Y. *J. Catal.* **2014**, *320*, 198−207.

(6) Bui, L.; Luo, H.; Gunther, W. R.; Román-Leshkov, Y. *Angew. Chem., Int. Ed.* **2013**, *52*, 8022−8025.

(7) Corma, A.; Domine, M. E.; Nemeth, L.; Valencia, S. *J. Am. Chem. Soc.* **2002**, *124*, 3194−3195.

(8) Corma, A.; Renz, M. *Angew. Chem., Int. Ed.* **2007**, *46*, 298−300.

(9) Corma, A.; Nemeth, L. T.; Renz, M.; Valencia, S. *Nature* **2001**, *412*, 423−425.

(10) Renz, M.; Blasco, T.; Corma, A.; Fornés, V.; Jensen, R.; Nemeth, L. *Chem. - Eur. J.* **2002**, *8*, 4708−4717.

(11) Snell, R.; Combs, E.; Shanks, B. *Top. Catal.* **2010**, *53*, 1248−1253.

(12) Holm, M. S.; Pagan-Torres, Y. J.; Saravanamurugan, S.; Riisager, A.; Dumesic, J. A.; Taarning, E. *Green Chem.* **2012**, *14*, 702−706.

(13) Dusselier, M.; Van Wouwe, P.; De Smet, S.; De Clercq, R.; Verbelen, L.; Van Puyvelde, P.; Du Prez, F. E.; Sels, B. F. *ACS Catal.* **2013**, *3*, 1786−1800.

(14) Corma, A.; Renz, M. *Chem. Commun.* **2004**, 550−551.

(15) Marakatti, V. S.; Halgeri, A. B.; Shanbhag, G. V. *Catal. Sci. Technol.* **2014**, *4*, 4065−4074.

(16) Corma, A.; Renz, M. *ARKIVOC* **2007**, *2007* (8), 40−48.

(17) Alarcón, E. A.; Correa, L.; Montes, C.; Villa, A. L. *Microporous Mesoporous Mater.* **2010**, *136*, 59−67.

(18) Selvaraj, M.; Choe, Y. *Appl. Catal., A* **2010**, *373*, 186−191.

(19) Mitchell, G.; Smith, S. C. Zeneca Limited, Patent No. US 5705456 A, January 6, 1998.

(20) Mulzer, J.; Mantoulidis, A.; Ohler, E. *J. Org. Chem.* **2000**, *65*, 7456−7467.

(21) Kagayama, T.; Sakaguchi, S.; Ishii, Y. *Tetrahedron Lett.* **2005**, *46*, 3687−3689.

(22) Henryon, V.; Monbrun, J.; Adisseo France S.A.S., Patent No. WO 2012049435 A1, April 19, 2012.

(23) Yamaguchi, S.; Motokura, K.; Sakamoto, Y.; Miyaji, A.; Baba, T. *Chem. Commun.* **2014**, *50*, 4600−4602.

(24) Román-Leshkov, Y.; Davis, M. E. *ACS Catal.* **2011**, *1*, 1566−1580.

(25) Ultraviolet−visible diffuse reflectance spectroscopy confirms the tetrahedral coordination of Sn in the zeolite framework. See also refs 4, 5 and 27.

(26) Chopade, S. P.; Sharma, M. M. *React. Funct. Polym.* **1997**, *34*, 37−45.

(27) Luo, H. Y.; Bui, L.; Gunther, W. R.; Min, E.; Román-Leshkov, Y. *ACS Catal.* **2012**, *2*, 2695−2699.

(28) Kohler, M. C.; Yost, J. M.; Garnsey, M. R.; Coltart, D. M. *Org. Lett.* **2010**, *12*, 3376−3379.

(29) Li, Y.-P.; Head-Gordon, M.; Bell, A. T. *ACS Catal.* **2014**, *4*, 1537−1545.

(30) Moliner, M.; Román-Leshkov, Y.; Davis, M. E. *Proc. Natl. Acad. Sci. U. S. A.* **2010**, *107*, 6164−6168.

(31) Centi, G.; van Santen, R. A. In *Catalysis for Renewables: From Feedstock to Energy Production*; Wiley-VCH Verlag GmbH & Co. KGaA: Weinheim, 2007; pp 27−28.

(32) Dusselier, M.; Van Wouwe, P.; de Clippel, F.; Dijkmans, J.; Gammon, D. W.; Sels, B. F. *ChemCatChem* **2013**, *5*, 569−575.

(33) Feather, M. S.; Harris, J. F. In *Advances in Carbohydrate Chemistry and Biochemistry*; Tipson, R. S., Derek, H., Eds.; Academic Press: New York, 1973; Vol. *28*, pp 161−224.

(34) Azofra, L. M.; Alkorta, I.; Elguero, J. *Carbohydr. Res.* **2013**, *372*, 1−8.

(35) Rasrendra, C. B.; Fachri, B. A.; Makertihartha, I. G. B. N.; Adisasmito, S.; Heeres, H. J. *ChemSusChem* **2011**, *4*, 768−777.

(36) Hayashi, Y.; Sasaki, Y. *Chem. Commun.* **2005**, 2716−2718.

(37) Taarning, E.; Osmundsen, C. M.; Yang, X.; Voss, B.; Andersen, S. I.; Christensen, C. H. *Energy Environ. Sci.* **2011**, *4*, 793−804.

(38) Bermejo-Deval, R.; Assary, R. S.; Nikolla, E.; Moliner, M.; Román-Leshkov, Y.; Hwang, S.-J.; Palsdottir, A.; Silverman, D.; Lobo, R. F.; Curtiss, L. A.; Davis, M. E. *Proc. Natl. Acad. Sci. U. S. A.* **2012**, *109*, 9727−9732.

(39) Román-Leshkov, Y.; Moliner, M.; Labinger, J. A.; Davis, M. E. *Angew. Chem., Int. Ed.* **2010**, *49*, 8954−8957.

(40) Delley, M. F.; Nuñez-Zarur, F.; Conley, M. P.; Comas-Vives, A.; Siddiqi, G.; Norsic, S.; Monteil, V.; Safonova, O. V.; Copéret, C. *Proc. Natl. Acad. Sci. U. S. A.* **2014**, *111*, 11624−11629.

(41) Crotti, A. E. M.; Fonseca, T.; Hong, H.; Staunton, J.; Galembeck, S. E.; Lopes, N. P.; Gates, P. J. *Int. J. Mass spectrom.* **2004**, *232*, 271−276.

(42) Geometries of all species were fully optimized at the B3LYP/6-31+G(d) level of theory using Gaussian 09 software.

(43) Assary, R. S.; Curtiss, L. A.; Dumesic, J. A. *ACS Catal.* **2013**, *3*, 2694−2704.

(44) Gunther, W. R.; Wang, Y.; Ji, Y.; Michaelis, V. K.; Hunt, S. T.; Griffin, R. G.; Román-Leshkov, Y. *Nat. Commun.* **2012**, *3*, 1109.

(45) Roland, J.; Avelino, C.; Marcelo Eduardo, D.; Rhodia Chimie Fr., Patent No. WO 2003064363, August 7, 2003.

(46) Mueller, L. L.; Griffin, G. L. *J. Catal.* **1987**, *105*, 352−358.

(47) Reuss, G.; Disteldorf, W.; Gamer, A. O.; Hilt, A. In *Ullmann's Encyclopedia of Industrial Chemistry*; Wiley-VCH Verlag GmbH & Co. KGaA: Weinheim, 2000; p 739.

(48) Clayden, J.; Greeves, N.; Warren, S. *Organic Chemistry*; Oxford University Press: New York, 2012; p 256.

(49) Ismalaj, E.; Strappaveccia, G.; Ballerini, E.; Elisei, F.; Piermatti, O.; Gelman, D.; Vaccaro, L. *ACS Sustainable Chem. Eng.* **2014**, *2*, 2461−2464.

(50) Aparicio, S.; Alcalde, R. *Phys. Chem. Chem. Phys.* **2009**, *11*, 6455−6467.

(51) Mellmer, M. A.; Sener, C.; Gallo, J. M. R.; Luterbacher, J. S.; Alonso, D. M.; Dumesic, J. A. *Angew. Chem., Int. Ed.* **2014**, *53*, 11872−11875.

(52) Luterbacher, J. S.; Rand, J. M.; Alonso, D. M.; Han, J.; Youngquist, J. T.; Maravelias, C. T.; Pfleger, B. F.; Dumesic, J. A. *Science* **2014**, *343*, 277−280.

(53) Van de Vyver, S.; Geboers, J.; Jacobs, P. A.; Sels, B. F. *ChemCatChem* **2011**, *3*, 82−94.